Quantized Spiral Tip Motion in Excitable Systems with Periodic Heterogeneities

Brent T. Ginn and Oliver Steinbock*

Department of Chemistry and Biochemistry, Florida State University, Tallahassee, Florida 32306-4390, USA

(Received 9 March 2004; published 8 October 2004)

Meandering spiral tips in homogeneous reaction-diffusion systems are characterized by two generically incommensurate radii and frequencies. Here, we create periodic perturbations in space to induce a transition to commensurate radii and frequencies that exhibit a devil's staircase. The plateaus of the staircase correspond to pinned or complex periodic orbits of the spiral tip.

DOI: 10.1103/PhysRevLett.93.158301 PACS numbers: 82.40.Ck, 05.45.–a, 82.20.Wt, 89.75.Kd

Vortices are observed in a variety of spatially extended systems. Examples include superconductors, Bose condensates, nonlinear optical media, and fluids with Rayleigh-Bénard flow [1]. Among nonequilibrium systems, reaction-diffusion (RD) media have contributed significantly to our understanding of these intriguing structures [2]. A major focus of current research is the external control of the wave patterns through periodic forcing [3], intricate feedback mechanisms [4], and spatial heterogeneities. The latter influence the dynamics of excitation vortices strongly and can give rise to anisotropic deformations of the global wave pattern [5]. Such phenomena are of particular interest because similar excitation waves exist in the intrinsically heterogeneous matter of living systems, such as cell colonies and cardiac and neuronal tissues [6].

In spatially homogeneous RD media, spiral tips describe circular or meandering trajectories [2,7]. The latter involve generically incommensurate frequencies and radii. In heterogenous systems that have obstaclelike areas, spirals are thought to be pinned to individual obstacle units. Examples for this behavior include Wiener and Rosenblueth's classic work on impulse conduction in cardiac muscle [8] and studies on spiral waves in chemical media [5,9]. In this Letter, we demonstrate that periodic heterogeneities can induce motion around numerous obstacle units. Moreover, the parameters of the tip trajectories are locked to values that are commensurate with the system's lattice constant yielding periodic orbits of finite length. These quantized orbits follow a devil's staircase [10] as the refractory period of the system is varied.

Our experiments employ the 1,4-cyclohexanedione Belousov-Zhabotinsky (CHD-BZ) reaction. This RD system involves the oxidation of an organic substrate by bromate in acidic solution and shows autocatalytic oxidation waves that are easily monitored under white light with a charged-coupled-device camera [11]. Following the preparation described in Ref. [12], we use soft lithography to create micropatterned reactor chips that are filled with the liquid CHD-BZ solution. The reactors are produced from the transparent elastomer poly(dimethylsiloxane) (PDMS) and sealed with a glass slide. The PDMS side of the reactor has a patterned surface relief that we designed as a gridlike array of intersecting channels. The width and height of the channels are both 200 μm. All obstacles are square and have an edge length of 800 μm. The CHD-BZ solution is prepared in nanopure water and employs the redox-catalyst $Fe[batho(SO_3)_2]_3^{4-/3-}$ at a concentration of 0.5 mmol/L. The initial concentrations of sulfuric acid, sodium bromate, and [1,4-cyclohexanedione] are varied, but always yield long induction times (4–6 h) during which the reaction remains in an unexcitable, oxidized state. Within the parameter range studied, spatially homogenous CHD-BZ systems show meandering spirals with large hypocyclic trajectories that cover areas of up to 40 mm^2 [13]. All experiments are carried out at room temperature.

Figure 1 shows an example of a spiral wave (white regions) propagating in a PDMS reactor. The overall pattern is fragmented and also deformed in vertical and horizontal directions according to the gridlike structure of the reactor. The spiral tip is not pinned to an individual PDMS obstacle, but rather rotates around two obstacle units that are marked with thin, black crosses. Notice that the tip has entered the channel between these two obstacles in the second frame. However, this particular wave segment fails to create a sustained rotation around the lower obstacle as it vanishes before exiting.

The trajectories of spiral tips depend strongly on the size of the obstacles, their overall geometry, and the initial concentrations of the reaction solution. Examples include rotation around 1, 1×2, and 2×2 obstacles. Figure 2(a) shows the resulting length d of the closed tip trajectories as a function of sulfuric acid concentration for three different concentrations of CHD. The discrete and periodic nature of the reactor geometry causes the locking of tip trajectories in certain permissible orbits. The longest trajectories are found for low concentrations of H_2SO_4 and CHD, whereas high concentrations give rise to simple pinning at single obstacles.

For lower initial concentrations, additional trajectories are observed, such as rotation around 1×3 obstacles. A typical example for this behavior is shown in Fig. 2(b), with the first five frames illustrating the main tip rotation

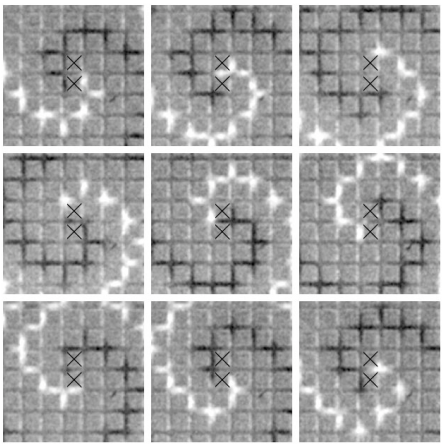

FIG. 1. Consecutive images of a counterclockwise rotating spiral wave in a micropatterned reactor. Individual frames are obtained by image subtraction yielding the bright (dark) areas where the oxidation (reduction) of the catalyst is fast. Over the entire sequence, the spiral tip performs one complete rotation around the two obstacles that are marked by thin crosses. Initial concentrations in mol/L: $[H_2SO_4] = 0.09$, $[NaBrO_3] = 0.50$, and $[CHD] = 0.20$. Time between frames: 25 s. Image area: (6.65×6.65) mm^2.

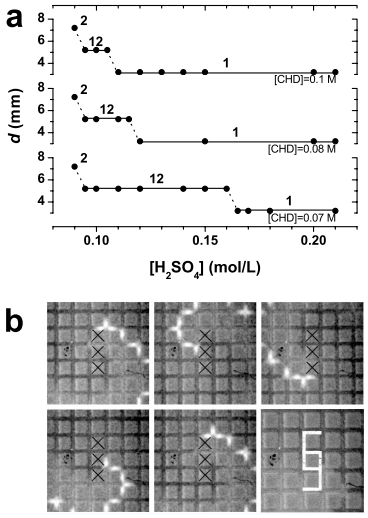

FIG. 2. (a) Length of spiral tip trajectories d as a function of sulfuric acid concentration for $[NaBrO_3] = 0.25$ mol/L. The corresponding trajectories result from rotation around 1, 1×2, and 2×2 obstacles, which we denote as "1," "12," and "2," respectively. (b) Five consecutive snapshots of a spiral wave rotating around 1×3 obstacle units (marked by black crosses). Time between frames: 75 s. Field of view: (6.12×6.12) mm^2. The sixth frame shows the resulting tip trajectory. Field of view: (5.0×5.0) mm^2. Initial concentrations in mol/L: $[CHD] = 0.05$, $[NaBrO_3] = 0.25$, and $[H_2SO_4] = 0.09$.

around the perimeter of the linear obstacle chain. This motion determines the frequency of the wave pattern (here 300 s). The spiral wave also enters the channels within the obstacle cluster similarly to the example shown in Fig. 1, which creates the discontinuous tip trajectory shown in the sixth frame of Fig. 2(b). Starting from the upper right corner of the trajectory, the tip moves one obstacle length to the left, two down, and then turns right to vanish at the next intersection. The next closest wave segment becomes the new tip. Originating at the lower left corner, it mirrors the path of the prior tip and completes the pattern.

To obtain more insight into the behavior of spiral waves in excitable systems with periodic heterogeneities, we carry out numerical simulations that mimic the essential features of our experiments. Our simulations employ Barkley's model [14] of excitable RD media, which involves a fast activator $u(x, y, t)$ and a slow inhibitor variable $v(x, y, t)$. We modify this model by introducing a control function $\Theta(x, y)$ that distinguishes excitable regions ($\Theta = 1$) from obstacles ($\Theta = 0$). To qualitatively model the loss of Br_2 and $BrO_2\bullet$ [12] into the PDMS matrix, the variables undergo simple exponential decay within the obstacle regions:

$$\frac{\partial u}{\partial t} = \nabla^2 u + \frac{\Theta}{\epsilon} u(1-u)\left(u - \frac{v+b}{a}\right) - (1-\Theta)u, \quad (1)$$

$$\frac{\partial v}{\partial t} = \delta \nabla^2 v + \Theta(u - v) - (1-\Theta)v. \quad (2)$$

The parameters δ, b, and ϵ are kept constant at 0.6, 0.005, 0.005, respectively, whereas a is varied between 0.16 and 0.6 to explore systems with different spiral tip dynamics. Our simulations are carried out for gridlike arrays in which the side length of the obstacles ($s_0 = 1.2$) equals the width of the individual channels (w_0).

Figure 3 shows nine consecutive snapshots of a spiral wave rotating around a pair of next-neighbor obstacle units. These obstacles are highlighted as white squares. The simulations show excellent agreement with the experimental data in Fig. 1. A minor difference between experiment and simulation concerns the wave segments that periodically enter the channel between the central obstacles. In the simulation, this process occurs twice per period and the wave segments vanish at the *midpoint* of the channel. We note that this symmetric motion is also observed in our experiments but for higher initial concentrations of CHD and $NaBrO_3$.

The simulations reveal a great variety of tip trajectories, some of which are illustrated in Fig. 4(a). To classify the trajectories, we introduce the following notation. We disregard wave segments that only probe channels but do not successfully exit. The resulting clockwise tip motion then describes a continuous path consisting of a repetitive sequence of horizontal and vertical lines. These straight lines involve motion along one, two, or more obstacle units. Consequently, we can describe simple pinning as "1," rotation around two obstacles as "12," and so on. The latter examples yield closed trajectories after four

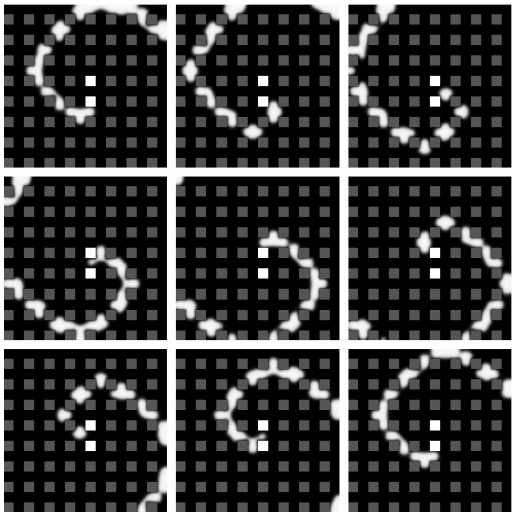

FIG. 3. Numerical simulation of a spiral wave based on Eqs. (1) and (2) using Euler integration and no-flux boundaries. The spiral tip rotates around a pair of obstacle units that are plotted in white. System length = 38.4; side length of obstacles $s_0 = 1.2$; model parameter $a = 0.25$; number of grid points = 512×512; time step $\Delta t = 10^{-3}$.

(i.e., "1111") and two repetitions ("1212") with lines that neither cross nor overlap. However, other trajectories such as "222131" do intersect and visit certain channels more than once before closing their path.

For each tip orbit represented by the sequence $n_1, n_2, \ldots, n_m$, one can compute the average length f of the straight lines constituting the pattern according to $f = -w_0 + (s_0 + w_0) \sum_{i=1}^{m} n_i/m$, where w_0 denotes the channel width. Notice that for a given wave velocity, the quantity f determines the excitation period far from the tip area. Figure 4(b) shows f/s_0 as a function of the model parameter a. The data reveal a devil's staircase with simple pinning for large values of a. For small a, we find long orbits that involve up to 25 obstacles as in the case of "225." The most pronounced plateaus correspond to the simple sequences "1," "112," "12," and "2." Three out of these four sequences are observed in our experiments. A preliminary survey of the tip dynamics in the (a, b)-parameter plane revealed numerous sequence bands. With increasing values of b, the more intricate sequences such as "222131" and the sequences with $f > 2s_0$ seem to vanish or become extremely thin.

Important conclusions can be drawn by comparing the devil's staircase in Fig. 4(b) with the dynamics of spiral waves in spatially homogeneous media. Figure 4(c) shows that the maximal and average radii of tip trajectories decrease with increasing values of a. For $a > 0.37$, we find periodic rotation around circular orbits. For smaller values, a supercritical Hopf bifurcation induces quasiperiodic tip dynamics along hypocycles [see inset of Fig. 4(c)], each of which is characterized by two frequencies (f_1, f_2) and radii (r_1, r_2) that are generically incommensurable [14]. We suggest that the devil's staircase in Fig. 4(b) is a *quantized* version of the smooth data shown in Fig. 4(c). This quantization is induced by the periodic heterogeneities and results in mode-locked, periodic tip trajectories. Similar to examples of devil's staircases in other systems [10], the length of the plateaus are generally wider for values of f/s_0 that are ratios of small integers.

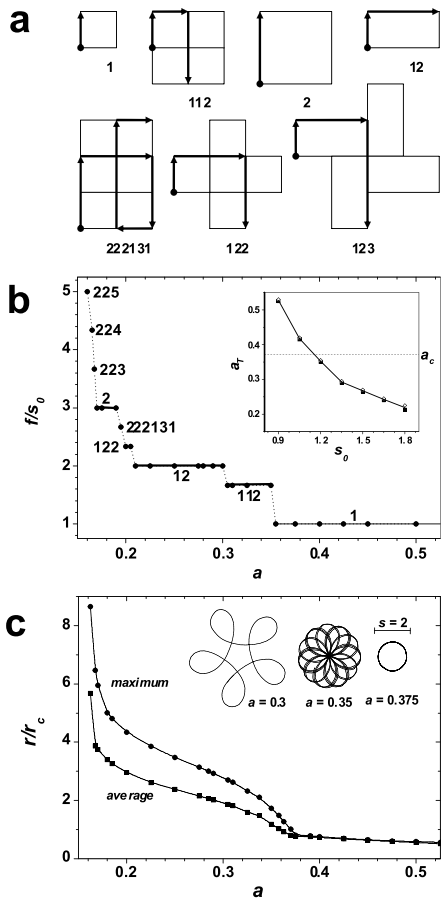

FIG. 4. (a) Schematic illustration of some spiral tip orbits. (b) Numerical results for the average step length f/s_0 of tip orbits as a function of the model parameter a. The inset shows the a value for "1" to "112" transitions as a function of the obstacle length s_0 for $s_0 = w_0$ with the dashed line indicating the Hopf bifurcation point of the homogeneous medium. (c) Maximal and average radii of spiral tip orbits in the homogeneous system for various values of a. The data are plotted as multiples of the radius $r_c = 0.8$ at the Hopf bifurcation point $a_c = 0.37$. The inset shows three representative tip trajectories.

Moreover, we find that the transition point a_T, at which simple pinning "1" changes to "112" motion, roughly coincides with the onset of meandering in the homogeneous system. However, the inset of Fig. 4(b) shows that a_T decreases monotonically with increasing values of s_0 and that a_T can differ significantly from the bifurcation point of the homogeneous medium (see dashed line). Consequently, circular tip motion in homogeneous

systems can give rise to compound motion around several obstacle units and meandering spirals can be pinned to single obstacles.

Despite this s_0-dependent shift of a_T, quasiperiodic meandering and quantized tip orbits in periodic reactor arrays share profound similarities. In both cases, the tip generates a refractory profile in its wake that controls its reentry and, in particular, forbids renewed excitation within the absolute refractory zone. For heterogeneous systems one can simplify this self-interaction and qualitatively discuss the breakdown of simple pinning: If the absolute refractory zone is shorter than the circumference of the obstacle, the tip is pinned to this particular obstacle. However, the tip is forced to select a different orbit of longer average length, if the size of the obstacles is decreased or if the length of the absolute refractory tail is increased (e.g., by decreasing the values of a or $[H_2SO_4]$). Hence, we expect that the average circumference of the quasiperiodic orbit for $a = a_T$ is similar to the perimeter of the individual obstacles and, for $s_0 = 1.2$, we indeed find these values as $2\pi r_0 = 5.7$ and $4s_0 = 4.8$.

In the framework of this simple discussion, we can approximate the spiral tip as an autonomous, chiral walker on a square lattice. The walker turns clockwise at every intersection if the channel (i.e., the bond) ahead has not been visited during the last n time steps. Otherwise it moves straight, thus avoiding the turn. This automaton generates trajectories such as "1" ($n \leq 3$), "112" ($4 \leq n \leq 6$), and "11213" ($7 \leq n \leq 8$). Moreover, we obtain the sequences "1," "12," "13," etc., if the critical refractoriness n is assigned to the nodes rather than to the bonds of the lattice. The resulting wealth of trajectories increases even further for chiral walkers on lattices with independent refractoriness of nodes and bonds. These simple models yield some agreement with our experimental and numerical findings but more importantly provide a qualitative understanding of the onset of multiobstacle motion and the devil's staircases in Figs. 2(a) and 4(b). However, the dynamics of spiral waves in RD systems are clearly more complex, because (i) the refractory tail is determined by the entire "arm" of the spiral wave and (ii) the tip motion is subject to curvature effects [15].

In conclusion, we have presented examples for quantized spiral rotation in RD systems with periodic heterogeneities. The experimental findings are reproduced by numerical simulations on the basis of a generic model for excitable media, thus indicating that the observed dynamics are characteristic for this class of systems. In particular, we believe that related phenomena exist in biological media, such as the interior of single cells and cell cultures [16], where nonexcitable structures, such as organelles or spatial variations in cell density, cause severe heterogeneities.

This work was supported by the National Science Foundation (NSF Grant No. CHE-20023105). We thank Thomas M. Fischer for discussions.

*Electronic address: steinbck@chem.fsu.edu

[1] K. Harada *et al.*, Nature (London) **360**, 51 (1992); J. R. Abo-Shaeer, C. Raman, J. M. Vogels, and W. Ketterle, Science **292**, 476 (2001); F. Huneus, B. Schapers, T. Ackemann, and W. Lange, Appl. Phys. B **76**, 191 (2003); B. B. Plapp, D. A. Egolf, E. Bodenschatz, and W. Pesch, Phys. Rev. Lett. **81**, 5334 (1998).

[2] *Chemical Waves and Patterns*, edited by R. Kapral and K. Showalter (Kluwer, Dordrecht, Netherlands, 1995).

[3] O. Steinbock, V. S. Zykov, and S. C. Müller, Nature (London) **366**, 322 (1993); V. S. Zykov, G. Bordiougov, H. Brandtstädter, I. Gerdes, and H. Engel, Phys. Rev. E **68**, 016214 (2003).

[4] O. U. Kheowan, V. S. Zykov, O. Rangsiman, and S. C. Müller, Phys. Rev. Lett. **86**, 2170 (2001); T. Sakurai, E. Mihaliuk, F. Chirila, and K. Showalter, Science **296**, 2009 (2002).

[5] O. Steinbock, P. Kettunen, and K. Showalter, Science **269**, 1857 (1995).

[6] B. Hess, Naturwissenschaften **87**, 199 (2000).

[7] D. Barkley, M. Kness, and L. S. Tuckerman, Phys. Rev. A **42**, 2489 (1990).

[8] N. Wiener and A. Rosenblueth, Arch. Inst. Cardiol. Mex. **16**, 205 (1946).

[9] O. Steinbock and S. C. Müller, Physica (Amsterdam) **188A**, 61 (1992); Phys. Rev. E **47**, 1506 (1993).

[10] B. Mandelbrot, *Fractals: Form, Chance, and Dimension* (Freeman, San Francisco, 1977); P. Bak and R. Bruinsma, Phys. Rev. Lett. **49**, 249 (1982); C. Reichhardt and F. Nori, Phys. Rev. Lett. **82**, 414 (1999).

[11] C. T. Hamik, N. Manz, and O. Steinbock, J. Phys. Chem. A **105**, 6144 (2001).

[12] B. T. Ginn, B. Steinbock, M. Kahveci, and O. Steinbock, J. Phys. Chem. A **108**, 1325 (2004).

[13] N. Manz, B. T. Ginn, and O. Steinbock, J. Phys. Chem. A **107**, 11 008 (2003).

[14] D. Barkley, Physica (Amsterdam) **49D**, 61 (1991).

[15] A. S. Mikhailov, *Foundations of Synergetics I* (Springer, Berlin, 1990).

[16] R. G. Worth, M. K. Kim, A. L. Kindzelskii, H. R. Petty, and A. D. Schreiber, Proc. Natl. Acad. Sci. U.S.A. **100**, 4533 (2003); S. M. Hwang, K. H. Yea, and K. J. Lee, Phys. Rev. Lett. **92**, 198103 (2004).